Supporting Information

Robust carbon-dots-based evaporator with enlarged evaporation area for efficient solar steam generation

Zhenzhen Wang,† Wenjing Tu,† Yajie Zhao, Hui Wang, Hui Huang, Yang Liu, Mingwang Shao*, Bowen Yao*, Zhenhui Kang**

1. Supplementary Methods

Materials

Graphite rods (99.99%) was purchased from Alfa Aesar Co., Ltd. Hydrazine hydrate were obtained from Chinasun Specialty Products Co., Ltd. Sodium chloride (NaCl) was purchased from Sinopharm Chemical Reagent Co., Ltd. All the reagents were tested directly without further treatment.

2. Supplementary Figures

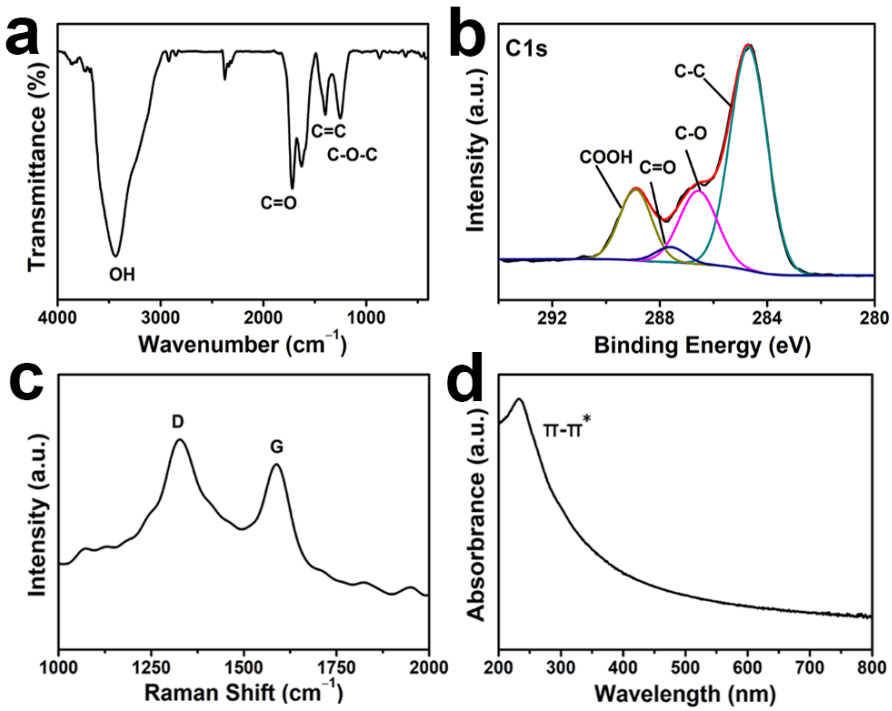

Figure S1. The structural characterizations of CDs. (a) FT-IR spectrum of CDs. (b) The high resolution C1s core level spectrum of CDs in XPS. (c) The Raman spectra (ex=633 nm) of the CDs. There were two prominent peaks at 1328 cm^{-1}, 1589 cm^{-1}, corresponding to the D and G peaks, as reported before. And the intensity ratio of the D band and G band (I_D/I_G) is a value to measure the disorder extent, along with the ratio of sp^3/sp^2 carbons. For as-prepared CDs, I_D is obviously higher than I_G, on account of the oxidation of graphite, and some structure defects appeared in the CDs, such as oxygenated groups (C–O, C=O) in the sp^2 carbon site, and then vacant lattice sites and sp^3 carbons were produced.[1] (d) The UV-vis absorption spectroscopy of CDs. The typical absorption peak at 233 nm showed the π-π^* transitions of C=C bond, which is in line with the results pointed out before.[2]

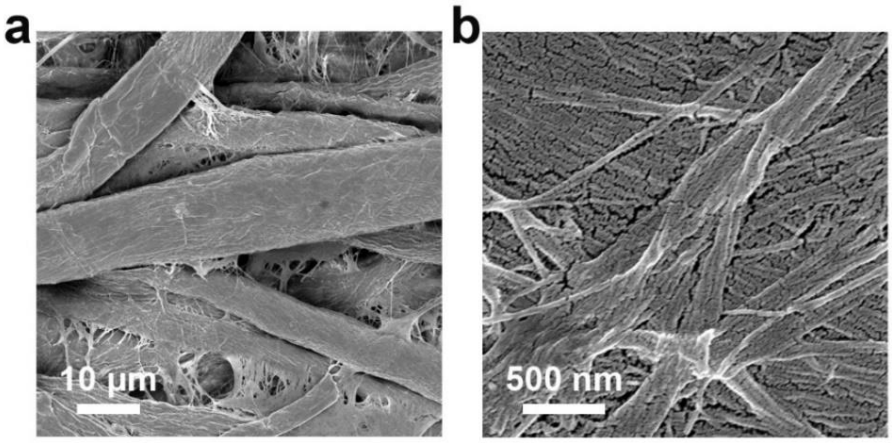

Figure S2. SEM images of cellulose paper.

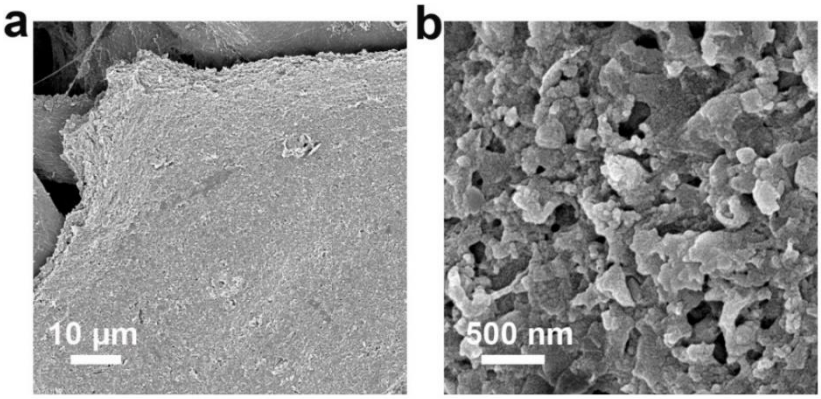

Figure S3. SEM images of CDE-2.

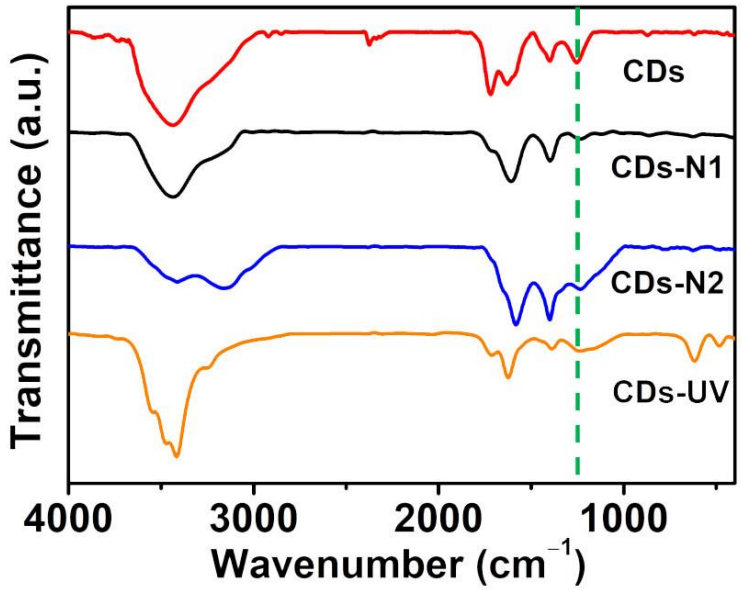

Figure S4. FTIR of CDs, CDs-N1, CDs-N2 and CDs-UV. Compared with CDs, it is evident that the peak of C-O was weaken for CDs-N1, CDs-N2 and CDs-UV, as green dotted line marked.

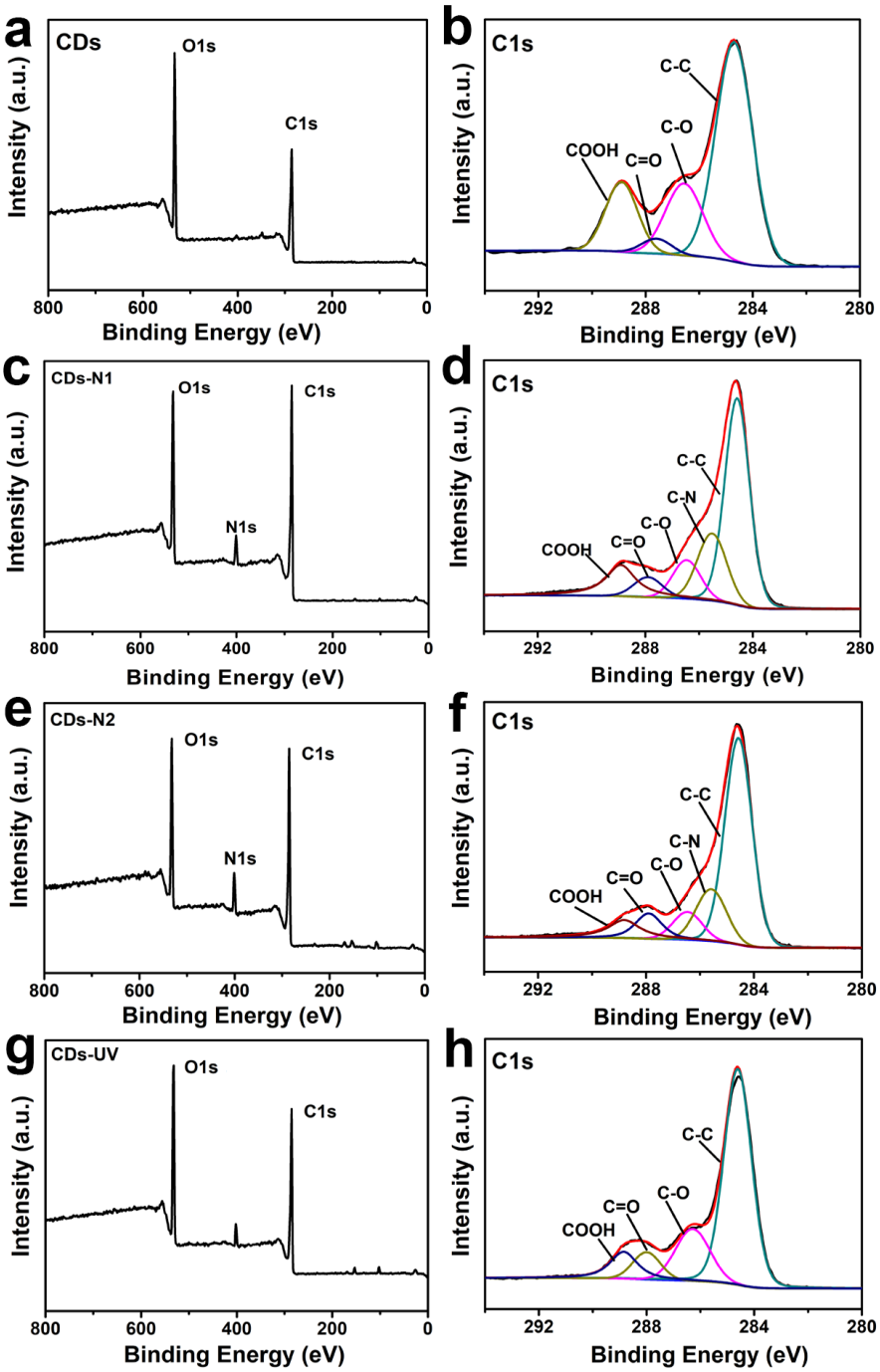

Figure S5. XPS full survey spectra and C1s spectra of (a)-(b) CDs, (c)-(d) CDs-N1, (e)-(f) CDs-N2, (g)-(h) CDs-UV.

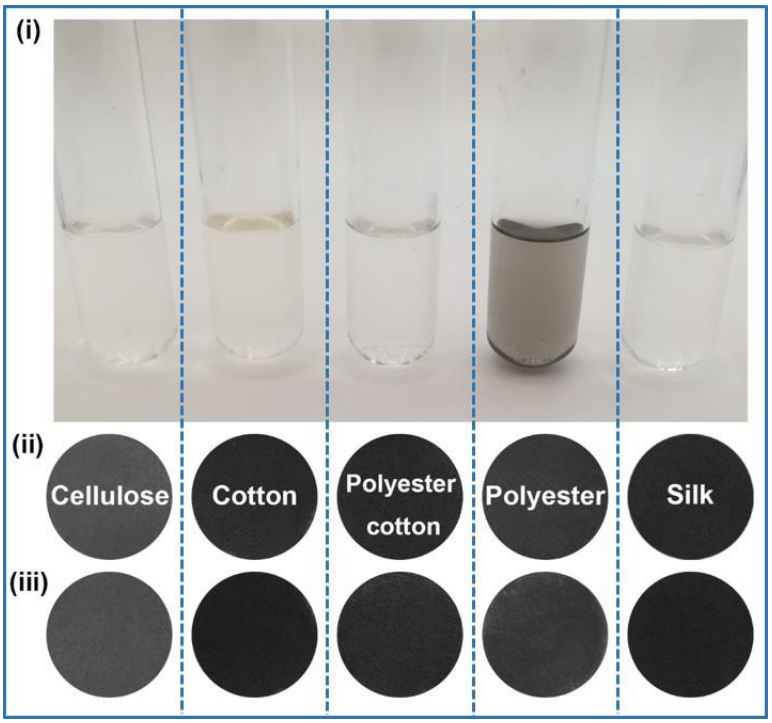

Figure S6. The change before and after 30 min ultrasonic treatment with varied absorbers. (i) The liquid left after ultrasonic, (ii) The absorbers with different substrates covered by carbon dots before ultrasonic, (iii) The different absorbers corresponding alignment after ultrasonic.

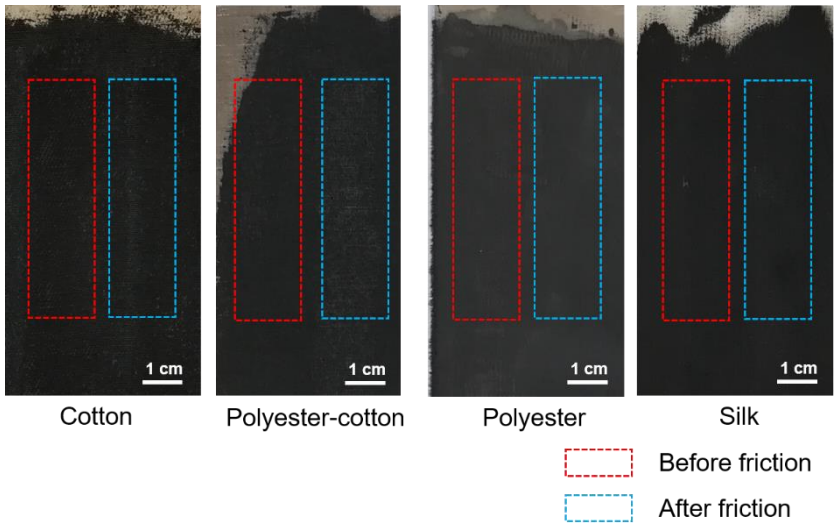

Figure S7. Wear resistance of CDs-based evaporators with various substrates(cotton, polyester-cotton, polyester, and silk) before and after friction.

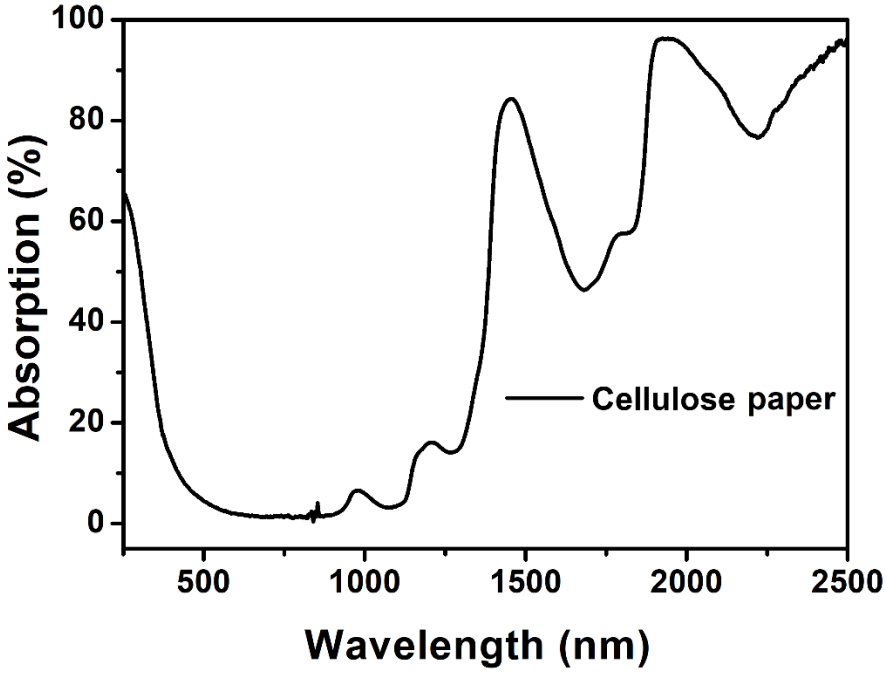

Figure S8. UV-vis NIR spectra of moist cellulose paper.

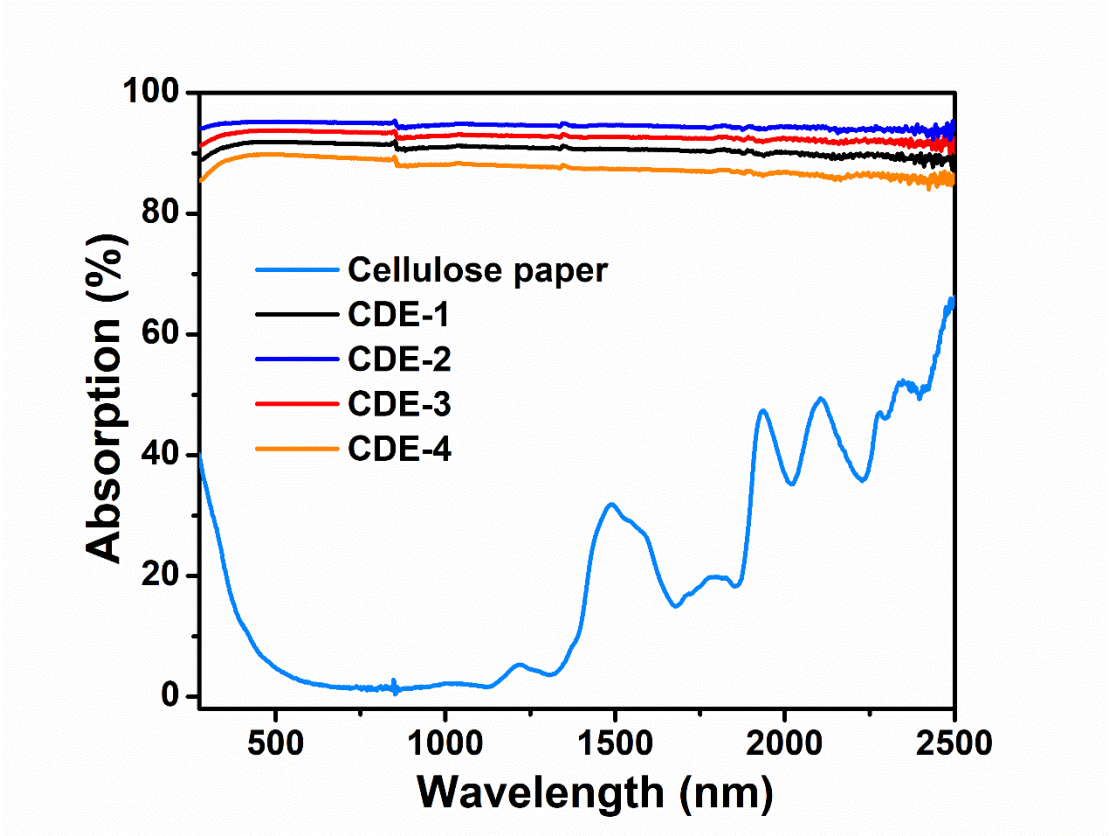

Figure S9 . UV-vis NIR spectra of dry CDE-1, CDE-2, CDE-3, CDE-4 and cellulose paper.

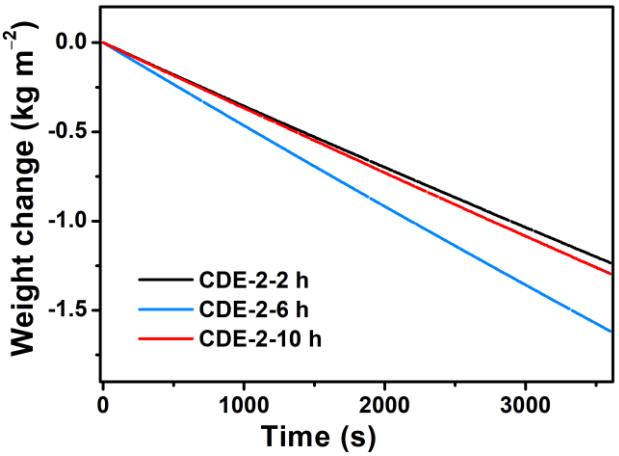

Figure S10. The mass change over time for CDE-2 with different thermal reduction time. CDE-2-2 h, CDE-2-6 h, CDE-2-10 h were covered with CDs-N1, which were treated by hydrazine after 2 h, 6 h and 10 h. And the mass changes of these solar stills were 1.23, 1.62, 1.29 kg m^{-2} h^{-1} under ambient temperature of 23.5 ℃, separately.

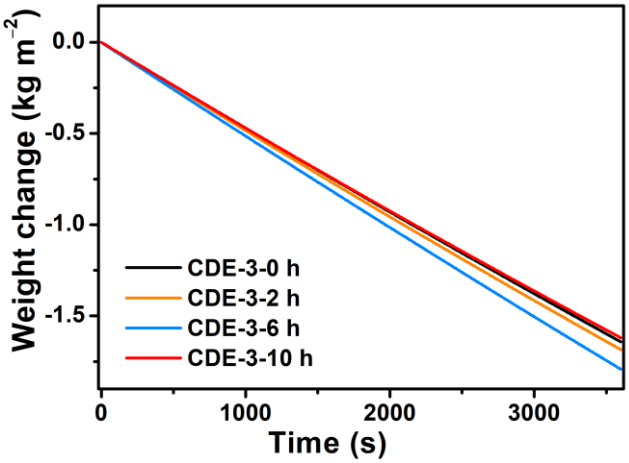

Figure S11. The mass change over time for CDE-3 with different reduction time. CDE-3-0 h, CDE-3-2 h, CDE-3-6 h and CDE-3-10 h, were gained after hydrazine treatment within 0 h, 2 h, 6 h and 10 h. And the mass changes of these solar stills were 1.64, 1.68, 1.79 and 1.62 kg m^{-2} h^{-1} under ambient temperature of 23.5 ℃, individually.

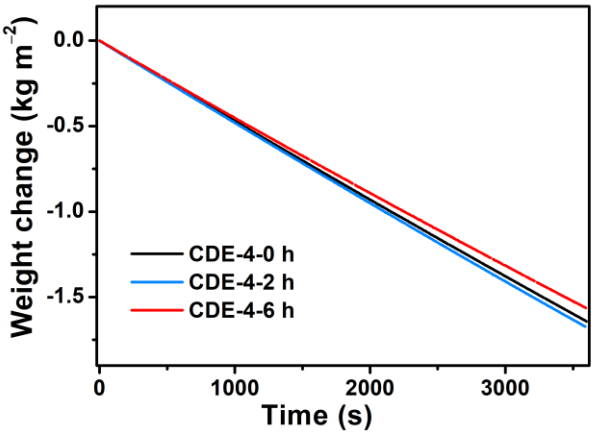

Figure S12. The mass change over time for CDE-4 with different UV light exposure time. CDE-4-0 h, CDE-4-2 h and CDE-4-6h were acquired after irradiation within 0 h, 2 h, and 6 h. And the mass changes of these solar stills were 1.64, 1.68, and 1.56 kg m^{-2} h^{-1} under ambient temperature of 23.5 ℃, individually.

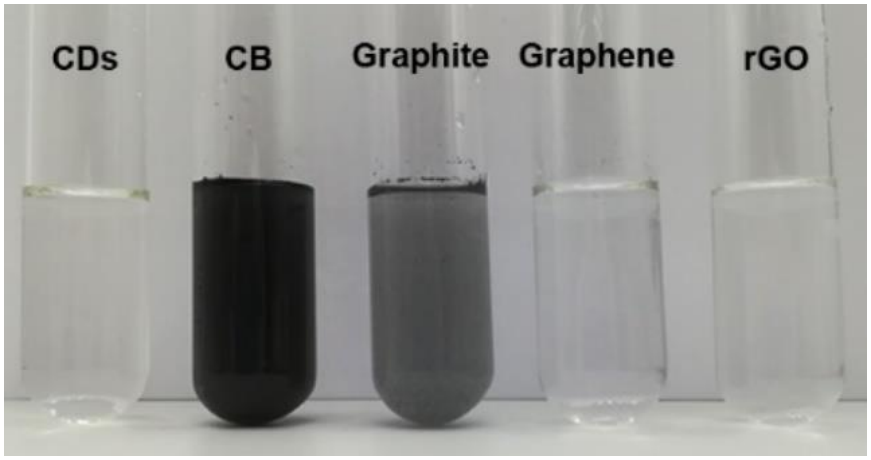

Figure S13. The photograph of the liquid left after 30 min ultrasonic treatment with varied absorbers.

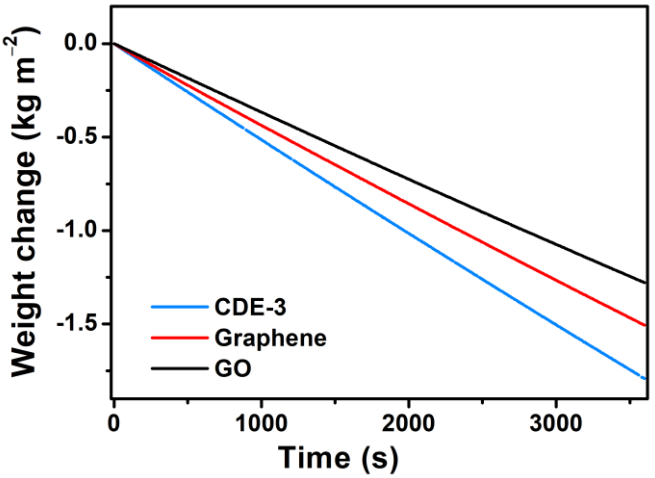

Figure S14. The mass change over time for CDE-3, graphene and GO under ambient temperature of 23.5 ℃.

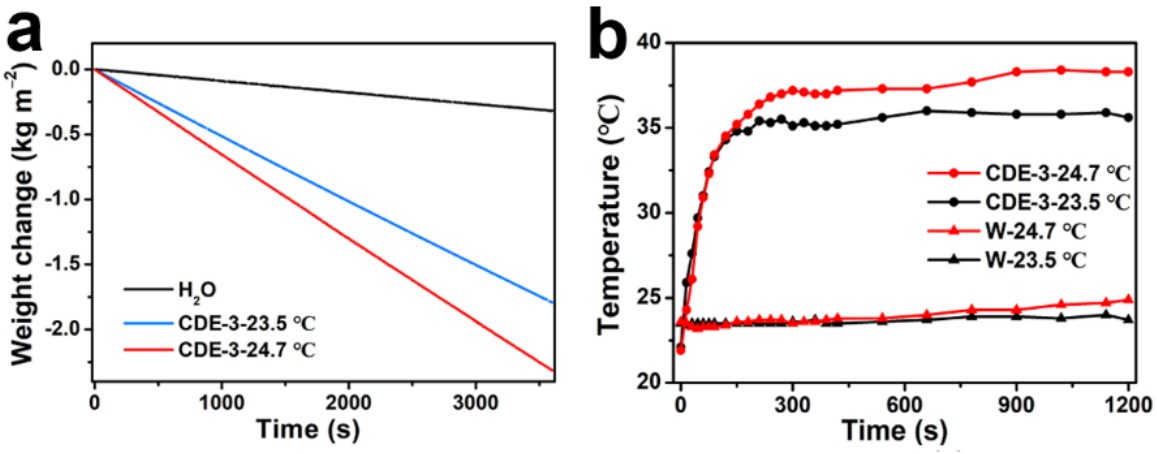

Figure S15. Under different ambient temperature, (a) The weight change with CDE-3. (b) Plot showing the temperature of bulk water and the surface of CDE-3 under 1 sun relative to irradiation time.

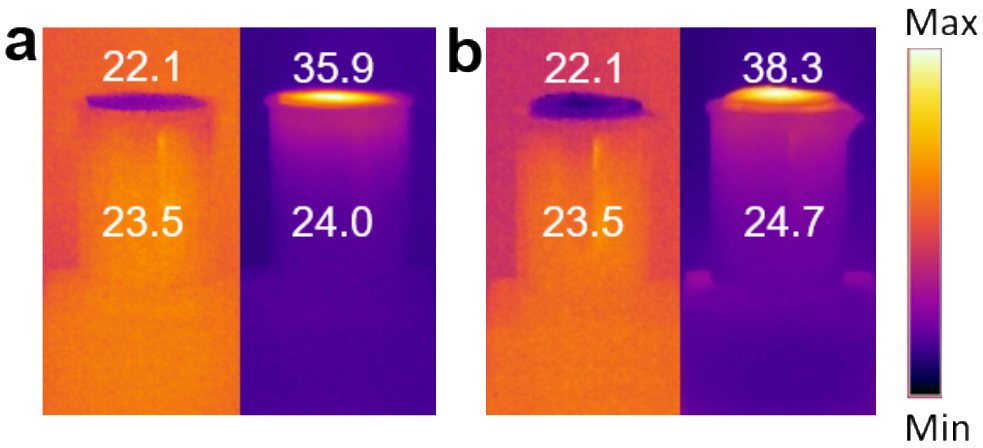

Figure S16. Infrared images of CDE-3 with light irradiation time of 0 min and 20 min under ambient temperature of (a) 23.5 ℃, (b) 24.7 ℃.

3. Supplementary Table

Table S1. The element contents and bond compositions from C1s spectra of CDs, CDs-N1, CDs-N2 and CDs-UV.

	CDs	**CDs-N1**	**CDs-N2**	**CDs-UV**
C content (at%)	67.08	70.78	67.59	69.86
O content (at%)	32.92	22.64	22.78	30.14
N content (at%)	-	6.58	9.63	-
C/O ratio	2.04	3.13	2.97	2.32
COOH (%)	16.62	13.33	8.76	10.17
C=O (%)	3.30	5.68	8.59	7.67
C-O (%)	20.10	10.39	8.24	18.22
C-N (%)	-	18.91	16.00	-
C-C/C=C (%)	59.99	51.68	58.41	63.94

Table S2. The comparisons of steam generation performance with carbon-based evaporators. (1 sun)

Materials	Evaporation rate ($kg\ m^{-2}\ h^{-1}$)	Preparation technique	Flexible	Robust	Reference
Graphene sheets membrane	1.62	Freeze-drying, annealing	×[b)]	×	3
Honeycomb graphene foam	1.30	Freeze-drying, annealing	×	×	4
3D porous graphene	1.50	CVD	×	×	5
CNT/GO + GO/NFC	1.25	3D-Printing	×	×	6
Carbon-coated paper	2.20	Solution impregnation	√[a)]	×	7
CB + PMMA + PAN	1.3	Electro -spinning	√	×	8
Cellular carbon sponge	1.39	Carbonization	×	√	9
Hollow carbon spheres	1.45	Gas-foaming	×	√	10
Carbon nanotube +filter paper	1.1	Solution impregnation	×	×	11
Carbonized melamine foams	1.270	Carbonization	×	√	12
Carbon fiber	1.47	Hydrothermal	√	√	13
Melamine-derived carbon sponges	1.98	Annealed	×	√	14
This work	2.31	Blade casting	√	√	

[a)] Does have this characteristic; [b)] Not have this characteristic.

4. Supplementary calculation

Theoretical analysis

The size of CDs is on the nanometer scale, while cellulose fiber the micron scale. Since there is a big difference between their sizes, fiber may be considered as a flat. And in the respect of symmetry of CDs, they may be modeled as cylinder with radius of R and height of H. And the cylinder is attached to the flat, the center of cylinder bottom is viewed as origin of 3D coordinates. Take vertically upwards as z axis, then the polar coordinate system is used to describe the point position of fiber surface, and the cylindrical coordinate system is applied to 3D coordinates, z = z (r, φ). Considering the shape of liquid film is unrelated to φ, this model could be simplified as quasi-two-dimensional coordinates, z = z(r). Here, surface area of a rotating body about z-axis symmetry:

$$S = 2\pi \int_0^{z_1} r\sqrt{1+(\frac{dr}{dz})^2}\,dz \tag{1}$$

Then the equation of liquid film, z=z(r), and meet the boundary conditions:

$$r = R, z = h, \frac{dz}{dr} = tg(\frac{\pi}{2}+\theta) = -ctg\theta$$

$$0 \le z \le H$$

Since CDs is only several nanometers, the neglect of gravity on liquid film may bring little effect. Then this question can be solved by variational approach. For the following function:

$$J[z,r] = \int_0^{z_1} F(r,r')dz = 2\pi \int_0^{z_1} r\sqrt{1+(\frac{dr}{dz})^2}\,dz \tag{2}$$

When it meets Eular equation, it reaches the extreme conditions.

$$F_r - \frac{d}{dz}F_{r'} = 0 \tag{3}$$

The solution to the Eular equation is:

$$z = K_2 - K_1 \ln(r + \sqrt{r^2 - K_1^{\,2}}) \tag{4}$$

where K1 and K2 are undetermined coefficients.

According to the boundary condition 1:

$$r = R, \frac{dz}{dr} = tg(\frac{\pi}{2}+\theta) = -ctg\theta$$

$$K_1 = R\cos\theta$$

And according to the boundary condition 2:

$$r = R, z_1 = h$$

$$K_2 = h + R\cos\theta \ln(R + \sqrt{R^2 - R^2\cos^2\theta})$$

So,

$$z = h + R\cos\theta \ln\frac{R(1+\sqrt{1-\cos^2\theta})}{r + \sqrt{r^2 - R^2\cos^2\theta}} \quad (5)$$

Then the surface area of liquid is:

$$S = 2\pi\int_0^{z_1} r\sqrt{1+(\frac{dr}{dz})^2}dz = 2\pi[\frac{r}{2}\sqrt{r^2 - K_1^{\,2}} + \frac{K_1^{\,2}}{2}\ln(r + \sqrt{r^2 - K_1^{\,2}})]_R^{r_2}$$

And the volume of liquid is:

$$V = \pi\int_0^{z_1} r^2 dz = K_1\pi[\frac{r}{2}\sqrt{r^2 - K_1^{\,2}} + \frac{K_1^{\,2}}{2}\ln(r + \sqrt{r^2 - K_1^{\,2}})]_R^{r_2}$$

$$S/V = 2/K_1 = 2/(R\cos\theta) \quad (6)$$

In cylindrical coordinate system, the height z is the signed distance from the chosen plane to the point A, the radial distance r is the Euclidean distance from the z-axis to the point A, and the azimuth φ is the angle between the reference direction on the chosen plane and the line from the origin to the projection of the point A on the plane. And in quasi-two-dimensional coordinates, z is the vertical distance from the origin as well. and r is the horizontal distance from the origin. S is the surface area of the formed liquid, V the volume of formed liquid, R is the radius of CDs, h is the signed distance from the chosen plane to the top of liquid, θ is the water contact angle of different absorbers, and H is the diameter of CDs.

5. Cost Analysis

This evaporator was easy to be manufactured at a low cost, promising for mass-produced applications and commercialization. From the estimate, the material cost of the floating solar still is around $ 1.67 for solar evaporator per square meter (including $ 0.14 for graphite rods, $ 0.06 for hydrazine hydrate, $ 0.20 for cellulose paper, $ 1.00 for floatable polystyrene (PS) foam, and $ 0.27 for gauze).

6. Supplementary References

1 H. Ming, Z. Ma, Y. Liu, K. Pan, H. Yu, F. Wang, Z. Kang, *Dalton Trans.*, 2012, **41**, 9526-9531.

2 H. Wang, H. Li, M. Zhang, Y. Song, J. Huang, H. Huang, M. Shao, Y. Liu, Z. Kang, *ACS. Appl. Mater. Inter.*, 2018, **10**, 16308-16314.
3 P. Zhang, J. Li, L. Lv, Y. Zhao, L. Qu, *ACS Nano*, 2017, **11**, 5087-5093.
4 Y. Yang, R. Zhao, T. Zhang, K. Zhao, P. Xiao, Y. Ma, P. M. Ajayan, G. Shi, Y. Chen, *ACS Nano*, 2018, **12**, 829-835.
5 Y. Ito, Y. Tanabe, J. Han, T. Fujita, K. Tanigaki, M. Chen, *Adv. Mater.*, 2015, **27**, 4302.
6 Y. Li, T. Gao, Z. Yang, C. Chen, W. Luo, J. Song, E. Hitz, C. Jia, Y. Zhou, B. Liu, B. Yang, L. Hu, *Adv. Mater.*, 2017, **29**, 1700981.
7 H. Song, Y. Liu, Z. Liu, M. H. Singer, C. Li, A. R. Cheney, D. Ji, L. Zhou, N. Zhang, X. Zeng, Z. Bei, Z. Yu, S. Jiang, Q. Gan, *Adv. Sci.*, 2018, **5**, 1800222.
8 W. Xu, X. Hu, S. Zhuang, Y. Wang, X. Li, L. Zhou, S. Zhu, J. Zhu, *Adv. Energy Mater.*, 2018, **8**, 1702884.
9 L. Zhu, M. Gao, C. K. N. Peh, X. Wang, G. W. Ho, *Adv. Energy Mater.*, 2018, **8**, 1702149.
10 J. Zhou, Z. Sun, M. Chen, J. Wang, W. Qiao, D. Long, L. Ling, *Adv. Funct. Mater.*, 2016, **26**, 5368-5375.
11 P. Yang, K. Liu, Q. Chen, J. Li, J. Duan, G. Xue, Z. Xu, W. Xie, J. Zhou, *Energy Environ. Sci.*, 2017, **10**, 1923-1927.
12 X. Lin, J. Chen, Z. Yuan, M. Yang, G. Chen, D. Yu, M. Zhang, W. Hong, X. Chen, *J. Mater. Chem. A*, 2018, **6**, 4642-4648.
13 T. Li, Q. Fang, X. Xi, Y. Chen, F. Liu, *J. Mater. Chem. A*, 2019, **7**, 586-593.
14 F. Gong, H. Li, W. Wang, J. Huang, D. Xia, J. Liao, M. Wu, D. V. Papavassiliou, *Nano Energy*, 2019, **58**, 322-330.